

# Nonlinear transport in $\beta$ - $\text{Na}_{0.33}\text{V}_2\text{O}_5$

S. Sirbu<sup>1</sup>, P.H.M. van Loosdrecht<sup>1</sup>, T.Yamauchi<sup>2</sup>, and Y. Ueda<sup>2</sup>

<sup>1</sup> Material Science Center, University of Groningen, 9747 AG Groningen, The Netherlands, e-mail: p.h.m.van.loosdrecht@rug.nl

<sup>2</sup> Institute for Solid State Physics, Tokyo University, Japan.

April 12, 2017

**Abstract.** Transport properties of the charge ordering compound  $\beta$ - $\text{Na}_{0.33}\text{V}_2\text{O}_5$  are studied in the temperature range from 30 K to 300 K using current driven DC conductivity experiments. It is found that below the metal-insulator transition temperature ( $T_{MI} = 136$  K) this material shows a nonlinear charge density modulation behavior. The observed conductivity is discussed in terms of a classical domain model for charge density modulation transport.

**PACS.** 71.30.+h Metal-insulator transitions and other electronic transitions – 72.20.Ht High-field and nonlinear effects – 72.80.-r Conductivity of specific materials

## 1 Introduction

There are many solid state materials which are one - dimensional and metallic at room temperature. Due to the coupling of the electrons to the underlying lattice the metallic state in these materials is usually not stable, leading to a phase transition into a charge modulated state at low temperatures. The low temperature ground state of the coupled electron-phonon system is characterized by a gap in the single-particle excitation spectrum, by collective modes formed by the electron-hole pairs, and by a deformation of the lattice. Many of those compounds are inorganic ( $\text{K}_{0.3}\text{MoO}_3$ ,  $\text{NbSe}_3$ ,  $\text{TaS}_3$ ) [2, 3, 1], but these properties are found in organic compounds as well (( $2.5(\text{OCH}_3)_2\text{DCNQI}$ )<sub>2</sub>Li, TTF-TCNQ) [4, 5]. The best known type of this class of phase transitions is the Peierls transition [6]. In this case the material develops the charge density modulation state at low temperature with a simultaneous deformation of the lattice, and the opening of a gap in the quasiparticle excitation spectrum. As long as the charge density modulation is pinned by lattice or impurities, these materials can be described as narrow-band-gap semiconductors or even insulators. An exception to this rule is  $\text{NbSe}_3$ , which remains a semimetal at low temperature [7]. One of the more intriguing features of low dimensional charge ordered materials are their nonlinear transport properties. In the charge density modulation ground state they only exhibit ohmic conductivity below a certain threshold applied electric field  $E_T$ . Below this field, the charge density modulation is pinned by lattice, impurities, defects, and grain boundaries and the conductivity is solely due to a strongly temperature dependent quasiparticle transport. For fields above  $E_T$ , the conductivity becomes strongly enhanced and nonlinear due to

the contribution of the now moving depinned charge density modulation [8, 9, 10, 11]. In addition to the nonlinear behavior, charge density modulated materials often show an alternating current response to a static applied field. This latter may be either due to so called ratcheting of the charge density modulation phase as observed in for instance  $\text{NbSe}_3$  [3], generally referred to as narrow band noise, or due to macroscopic polarization oscillations as observed in for instance blue bronze at low temperatures [12].

The recently revived interest in the vanadium bronze  $\beta$ - $\text{Na}_{0.33}\text{V}_2\text{O}_5$  has been triggered by the observation of a charge ordering transition [13], and sparked once more by the observation of the pressure induced superconductivity [14] in this electronically low dimensional material. The vanadium bronze  $\beta$ - $\text{Na}_{0.33}\text{V}_2\text{O}_5$  has been the subject of various structural studies during the last 40 years [15, 16]. At room temperature  $\beta$ - $\text{Na}_{0.33}\text{V}_2\text{O}_5$  is a highly anisotropic metal with a site occupancy disorder of the sodium atoms. Around  $T_{Na} = 240$  K a second order phase transition occurs leading to an ordering of the sodium atoms and a doubling of the primitive cell along the b direction [17]. A charge ordering transition, which is thought to be driven by the electron phonon coupling, occurs at  $T_{MI} = 136$  K and is accompanied by a further tripling of the unit cell along the b direction [17, 18], leading to a commensurate charge modulated state with a period of 6b. Temperature dependent measurements of the magnetic susceptibility revealed a magnetic transition from a paramagnetic to an antiferromagnetic state at  $T_{AF} = 22$  K [13]. Finally, as mentioned above,  $\beta$ - $\text{Na}_{0.33}\text{V}_2\text{O}_5$  becomes a superconductor for pressures above 8 GPa and low temperatures (8 K) as revealed by recent pressure dependent resistivity measurements [14]. Optical conductivity data

suggest that this system may be understood in terms of a small polaron model, where the charge ordering in fact corresponds to an ordering of the polarons [19,20]. Since previous experiments strongly suggest that  $\beta$ - $\text{Na}_{0.33}\text{V}_2\text{O}_5$  is a low dimensional conductor with an electron-phonon interaction induced charge ordering, this material should also show the usual nonlinear transport properties discussed above. Indeed the results presented in this paper of the first detailed measurements of the field dependence of conduction in the sodium bronze  $\beta$ - $\text{Na}_{0.33}\text{V}_2\text{O}_5$  are fully consistent with this picture. The observed nonlinear transport properties are well described using a classical domain model. The observed charge density modulation conductivity increases with increasing temperature, suggesting a screening of the charge density modulation pinning by the thermally excited carriers.

## 2 Temperature dependent transport

Single crystal samples have been prepared as described elsewhere [17]. Platelets with typical dimensions  $4 \times 2 \times 0.2 \text{ mm}^3$  were mounted on the cold finger of a flow cryostat and contacted using  $50 \mu\text{m}$  diameter platinum wires. Four wires were fixed on the sample surface using silver paste, spaced 1 mm apart. Measurements were performed along the b axis in a four probe configuration using a Keithley 236 source-meter in a current driven mode. The resistivity was calculated from the measured resistance and the geometry of the sample.

First we turn to the temperature dependence of the low-field ohmic resistance, of which a typical example is shown in Fig.1 [21]. The strong increase of the resistivity below  $T_{MI} = 136 \text{ K}$  clearly signals the charge ordering transition, consistent with results published in literature. Note that also the sodium ordering transition at  $T_{Na} = 240 \text{ K}$  leads to a change in the temperature dependence of the resistivity (see also inset Fig. 1.). The small enhancement of the conductivity below  $T_{Na}$  can be understood in terms of the decreased amplitude of the spatial potential variations on the vanadium sites due to the ordering of the sodium subsystem [19]. Although the resistivity at high temperatures ( $T > T_{MI}$ ) is fairly small, as expected for a bad metal, it does not exhibit the metallic behavior as observed previously [17]. The reason for this could be that the samples are slightly misaligned. In this case the measured resistivity is a combination of the resistivity of the metallic b-axis and the insulating perpendicular axes, leading to the observed temperature dependence. X-ray diffraction experiments on the samples, however, have ruled out this option in showing that to within a degree the samples are indeed b-oriented. A more likely reason is that the sodium stoichiometry of the sample slightly deviates from  $x = 0.33$ , which is known to lead to a rapid loss of metallic behavior and eventually to the disappearance of the metal-insulator transition [13]. Such deviations lead to an additional disorder in the sodium site occupancy, which in turn leads to a more disordered potential on the vanadium sites which make up the one-dimensional conduction chains [19]. Since in particular low

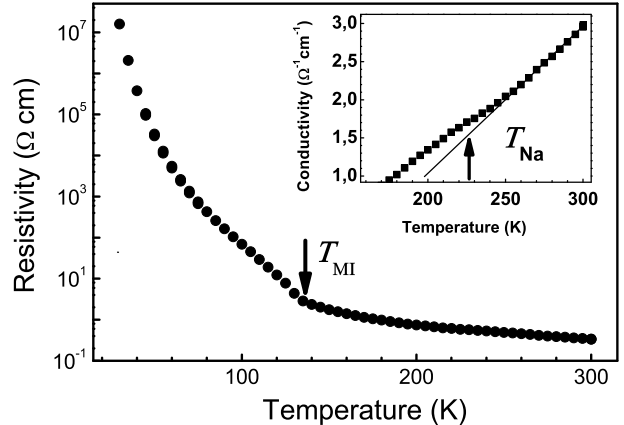


**Fig. 1.** Resistivity as a function of temperature in  $\beta$ - $\text{Na}_{0.33}\text{V}_2\text{O}_5$ . Inset: change in conductivity near the sodium ordering transition at  $T_{Na} \simeq 240 \text{ K}$ .

dimensional systems are very susceptible to disorder, this may lead to a small disorder induced gap and to the observed non-metallic behavior.

An estimate for the transport gaps above and below the charge ordering transition temperature is obtained fitting a simple activated behavior,  $\rho = \rho_0 \exp(\Delta/kT)$ , to the data. Well within the charge ordered phase ( $30 \text{ K} \leq T \leq 80 \text{ K}$ ) we find  $\rho_0 = 630 \text{ m}\Omega\text{cm}$  and a gap  $\Delta_{LT} = 548 \text{ K}$ . At high temperatures ( $150 \text{ K} \leq T \leq 300 \text{ K}$ ) we find  $\rho_0 = 75 \text{ m}\Omega\text{cm}$  and a gap  $\Delta_{HT} = 472 \text{ K}$ . Surprisingly, the transport gap in the charge ordered phase is only about 15% larger than the one found for the high temperature phase. The major change is found in the prefactors which differ by an order of magnitude. This is consistent with the expectation that the majority of the charge carriers is frozen out by the charge ordering at  $T_{MI}$ . In a similar analysis Yamada *et al.* [13] found an activation energy of 538 K, in good agreement with the present value. In previous work we found an optical gap of  $2\Delta = 2450 \text{ K}$  [19]. Most likely, this optical gap corresponds to the energy needed to free a quasiparticle from the charge ordered state. Clearly then, the transport gap must have a different origin. The origin for this difference could be that the observed transport gap is in fact a sodium disorder induced pseudo gap in the charge carrier spectrum, where the charge carriers themselves are present due to an incomplete charge ordering, rather than due to thermal excitation as is usually the case. This would be consistent with the small difference in the transport gap values below and above the charge ordering transition, as well as with the observed finite low frequency conductivity in the optical data [19].

However, closer inspection of the low temperature conductivity shows that it does not strictly follow an activated behavior. In particular, below 60 K there seems to be an enhancement of the conductivity, which presumably is due to the presence of an additional conductivity channel. In a purely one-dimensional model, such an enhancement may originate from the presence of mid-gap bound states of

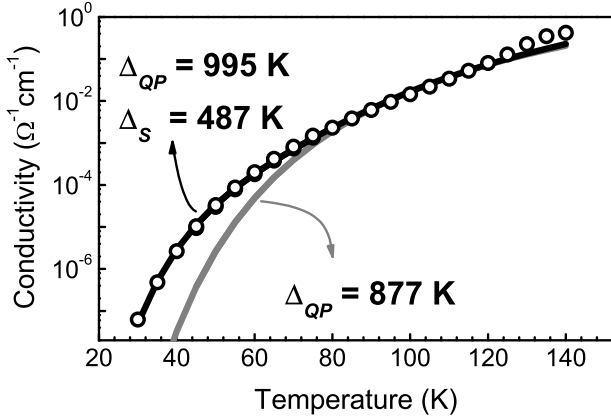


**Fig. 2.** Temperature dependent conductivity (symbols, same data as in Fig. 1.) together with a fit to an activated two particle behavior, Eq. (1) (dark line). The gray line shows a fit of thermally activated quasiparticle transport to the high temperature part of the data.

amplitude  $\pi$ -solitons and quasiparticles, as described by Brazovskii [22]. Indeed, the low temperature conductivity is better described by the empirical form

$$\sigma(T) = \sigma_{QP}^0 \exp(-\Delta_{QP}/kT) + \sigma_S^0 \exp(-\Delta_S/kT). \quad (1)$$

Here the first term on the right hand side accounts for the contribution of the quasiparticles, whereas the second term takes the midgap state conductivity into account. In the *one*-dimensional description, the midgap states are located halfway the quasiparticle gap, *i.e.*  $\Delta_S \approx \Delta_{QP}/2$ . Fitting Eq. (1) to the data yields  $\Delta_{QP} = 995$  K;  $\Delta_S = 487$  K, and a ratio  $\sigma_{QP}^0/\sigma_S^0 \sim 0.4 \times 10^3$ . Note that the quasiparticle gap obtained in this way becomes comparable to the gap found in optical experiments [19]. The conductivity ratio shows that just below the phase transition quasiparticle transport dominates the conductivity, whereas the ‘midgap’ contribution becomes important at lower temperatures only, despite its smaller energy gap. Finally, we note that a similar analysis to blue bronze,  $\text{K}_{0.3}\text{MoO}_3$ , data leads to similar conclusions. For both these cases, one can worry whether a one-dimensional model is applicable at all. Indeed, the midgap states described by Brazovski require the existence of topological  $\pi$ -solitons which do not exist in three dimensions. Therefore, the above analysis merely shows the presence of additional excitations halfway the gap. Though in sodium vanadate, these might originate from the sodium disorder, one would not expect a similar disorder in blue bronze. Therefore, the precise nature of the midgap states remains unresolved at present. One interesting thought is that they might result from excitations inside domain walls which separate the charge density modulation ordered regions in the samples.

### 3 Field dependent transport

The charge density modulation in low dimensional systems is usually pinned by the underlying lattice, by impurities or by structural defects. When the charge density modulation is incommensurate with the underlying lattice, the main pinning centers are the impurities and other defects. In this case, the pinning might be considered relatively weak, and the charge density modulation can fairly easily move in the material upon application of an external electric field, leading to the typical non-linear charge density wave conduction. When the modulation is commensurate with the lattice, the pinning is considered to be strong, usually much stronger than the impurity pinning, and the large pinning energy prevents conduction of the charge density modulation. The charge modulation in  $\beta$ - $\text{Na}_{0.33}\text{V}_2\text{O}_5$  is commensurate with the underlying lattice. Since the modulation period is, however, rather large (6b) the commensurability pinning in this system is expected to be relatively weak, opening the possibility of non-linear charge density wave conduction in the charge ordered phase.

To study the nonlinear transport properties of single crystal  $\beta$ - $\text{Na}_{0.33}\text{V}_2\text{O}_5$ , current driven field dependence measurements [23] were performed in the temperature range 65 K - 300 K. The obtained transport properties are very similar with those obtained in CDW systems. A typical example of the conductivity measured along the b-axis at 65 K is displayed in Fig. 3.

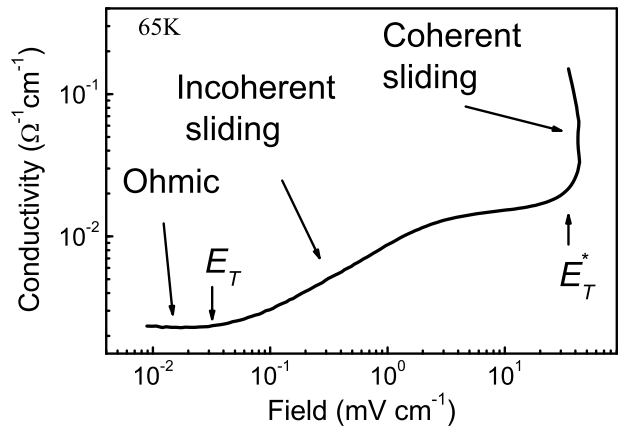


**Fig. 3.** Nonlinear field dependent conductivity in  $\beta$ - $\text{Na}_{0.33}\text{V}_2\text{O}_5$  measured along the b axis at 65 K displaying three charge density modulation transport regimes.

The behavior of the conductivity shows three regimes. Below 0.06 mV/cm (first threshold field) the conductivity is field-independent and mainly due to quasiparticle transport. At about 0.06 mV/cm the conductivity shows a nonlinear increase resulting from an incoherent contribution of the charge density wave to the conductivity. This behavior saturates around 4 mV/cm. Above the second threshold field at 30 mV/cm a step increase of the con-

ductivity takes place signaling the onset of the coherent charge density modulation regime. Despite the strong increase of the conductivity, it never reaches values comparable to the metallic state.

The values for the threshold fields are smaller than those found, for example in blue bronze. Zawilski *et al.* [11] reported 40 mV/cm for the first threshold field and around 2000 mV/cm for the second threshold field in  $\text{K}_{0.3}\text{MoO}_3$  at 60 K while Mihaly *et al.* [24] found 40 mV/cm in  $\text{K}_{0.3-x}\text{Na}_x\text{MoO}_3$  around the same temperature. Fleming *et al.* [25] found the first threshold field around 500 mV/cm in  $\text{TaS}_3$  and 90 mV/cm in  $\text{K}_{0.3}\text{MoO}_3$  both measured at 60 K. In  $\text{K}_{0.3-x}\text{Na}_x\text{MoO}_3$  ( $x = 0, 0.02, 0.05, 0.1$ ), at 77 K, Wang *et al.* [26] reported values of (300, 670, 750, 950) mV/cm for the first threshold field at 180 K. Beauchene *et al.* [27] reported similar values in  $\text{Rb}_{0.3}\text{MoO}_3$ . Küntscher *et al.* [28] found in  $\text{K}_{0.3}\text{MoO}_3$  and  $\text{Rb}_{0.3}\text{MoO}_3$  values of 150 mV/cm for the first threshold field at 60 K while van Loosdrecht *et al.* [10] found 200 mV/cm at the same temperature. Although the values of the first threshold field for  $\text{K}_{0.3}\text{MoO}_3$  show some variation, they are typically in the 50-200 mV/cm range, *i.e.* substantially higher than the present values observed for  $\beta$ - $\text{Na}_{0.33}\text{V}_2\text{O}_5$ . This is consistent with the notion that the temperature dependence of the low field transport observed in  $\beta$ - $\text{Na}_{0.33}\text{V}_2\text{O}_5$  is due to incomplete charge ordering resulting from disorder in the sodium sublattice. The presence of charge carriers, even at low temperatures, leads to screening of the pinning potential, and hence to a lowering of the threshold field. In contrast, the presence of charge carriers in blue bronze is almost entirely due to thermal quasiparticle excitations.

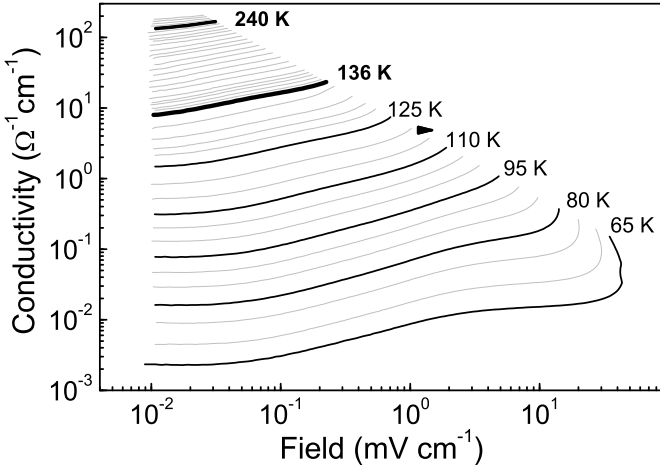


**Fig. 4.** Nonlinear conductivity along the b axis as a function of electric field in  $\beta$ - $\text{Na}_{0.33}\text{V}_2\text{O}_5$  measured from 65 K to 300 K (in 5 K steps between 65 K - 125 K, 140 K - 230 K, and 250 K - 300 K; in 2 K steps in the transition temperatures regions: 128 K - 146 K, and 236 K - 246 K).

Figure 4 displays the electric field dependence of the conductivity along the b-axis for a variety of temperatures between 65 K and 300 K. The nonlinear behavior

is most pronounced at low temperatures, and is slowly decreasing upon increasing the temperature towards the transition temperature  $T_{MI}$ . The first threshold field  $E_T$ , *i.e.* the field required to induce charge density modulation conductivity, is observed below  $T_{MI}$  only. As the temperature is reduced, the threshold fields increase, evidencing a strengthening of the charge density modulation pinning. This is due to the reduction of the free carrier concentration at lower temperatures, leading to a less effective screening of pinning centers. The second transport regime, the incoherent moving regime, shows an increasing conductivity followed by saturation upon increasing field. Going up in temperature, the field at which this saturation is reached increases, until around 90 K it merges with the second threshold field.

Even above the charge ordering transition temperature, the nonlinear behavior has not entirely disappeared, although there are no clear threshold fields anymore. Nonlinear conduction is still observed up to the sodium ordering temperature  $T_{Na} = 240$  K, consistent with the disorder induced non-metallic behavior observed above  $T_{MI}$ . Finally, above 240 K a nearly field independent conductivity is observed.

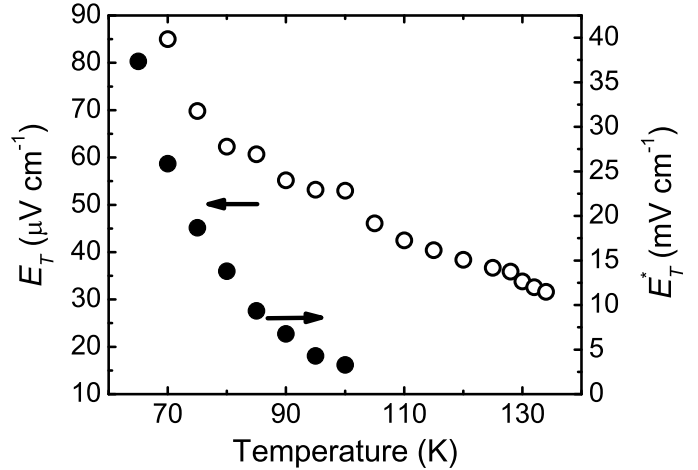


**Fig. 5.** Temperature dependence of the threshold fields for  $T < T_{MI}$ , obtained from the conductivity data. Open symbols (left scale): first threshold field; Filled symbols (right scale): second threshold field.

The temperature dependencies of the first and second threshold fields are shown in Fig. 5. The open symbols display the first threshold field,  $E_T$ , obtained from the conductivity curves by taking the values where the conductivity starts to increase. The lower part displays the second threshold field,  $E_T^*$ , obtained in a similar manner. Although there is a factor of  $10^3$  difference between the two threshold fields, the displayed behavior is qualitatively the same: the threshold field strongly decreases with increasing temperature. With some exceptions ( for example  $\text{K}_{0.3}\text{MoO}_3$  or  $\text{TaS}_3$  [29] ) this type of behavior for in particular the first threshold field is common for many of the known charge density wave systems. At low tempera-

ture, when the number of quasiparticles is reduced, large electric fields may build up around pinning centers and the value of  $E_T^*$  is essentially determined by the amount of disorder in the system. Going up in temperature, the thermally excited quasiparticles tend to homogenize the electric field inside the sample. This effect is a natural source for the redistribution of the driving fields inside the sample.

A variety of models were proposed to describe the nonlinear conductivity observed in charge density modulation materials, mostly based on the original suggestion of Fröhlich [30] that conductivity is dominated by sliding CDW transport. Between them, there are two main approaches in describing the CDW conductivity [1,9,31]. The first one, treats the CDW as a classical particle which is moving in a periodic potential, with the period determined by the period of the CDW [32,33]. This model gives a sharp threshold field,  $E_T$  for the onset of nonlinearity and a saturation of the conductivity for high electric fields. The second model, proposed by Bardeen and referred to as the tunneling model [34], assumes that the nonlinear transport occurs as a result of coherent tunneling of the CDW over macroscopic distances. Besides the threshold field,  $E_T$ , the model gives another characteristic field  $E_0$ , which can be interpreted as a tunneling barrier. The onset of the conductivity reveals a sharp threshold field and at high electric fields the conductivity saturates. Both models rely on a  $T = 0$  treatment of the problem, though nonzero temperature models based on thermally assisted flux creep have been discussed as well [35,31]. The models described above fail to account for the charge density modulation conductivity observed in  $\beta$ - $\text{Na}_{0.33}\text{V}_2\text{O}_5$ . Fukuyama, Lee and Rice [36,37] discussed the effect of the pinning centers on the charge-density-waves dynamics. They focused on phase fluctuations and show that, when the material is characterized by weak pinning, the system can be thought to break up into domains. Here, we integrate this notion in a simple phenomenological model describing the observed nonlinear transport in  $\beta$ - $\text{Na}_{0.33}\text{V}_2\text{O}_5$ , by treating the sample as a collection of interconnected domains. Each domain is characterized by its own conductivity and threshold field so that the sample can be considered as a collection of parallel and series nonlinear conduction paths. At low applied fields (smaller than  $E_T$ ), excited quasiparticles dominate the conductivity of a single domain, leading to the strongly temperature dependent ohmic behavior. All charge density modulation domains are pinned by lattice and defects and will not start moving until the applied field exceeds a certain critical field. At higher applied fields, some domains start to become depinned, leading to an additional charge density modulation contribution to the conductivity. The charge density modulation still cannot move as a whole due to the domain structure resulting from grain boundaries and strong pinning centers. The sample is now in the incoherent moving regime. Finally for applied fields exceeding a second critical field, the charge density modulation may move as a whole (or at least a percolation path exists between the contacts), and the conductivity becomes com-

pletely dominated by the moving charge density modulation transport. Within this model, the second critical field is then a percolation threshold and the transport regime above this field is dubbed coherent moving regime.

The model sketched above can be made more quantitative by specifying a model for the charge density modulation conductivity itself. Here we take one of the simplest approaches, and describe the charge density modulation within a domain as a charged particle moving due to an applied field  $E$  in a viscous medium [1]. The charge density modulation conductivity is then given by.

$$\sigma_{cdm}(E) = \sigma_c \frac{E - E_T}{E} \theta(E - E_T), \quad (2)$$

where the Heaviside function  $\theta(E - E_T)$  assures that the equation is also valid for  $E < E_T$ . In the incoherent moving regime the conductivity can then be modeled as a collection of interconnected charge density modulation domains, shunted by the free carrier conductivity. In general, this is still a complex system which solution would require detailed knowledge of domain properties and their connectivity. Here we will take a more qualitative and statistical approach, and model the charge density modulation system as a statistically large number of interconnected domains. The conductivity of this network of domains together with the free carrier conductivity will then yield the total conductivity. The network can be considered as a collection of parallel and series conduction paths. For the series connected domains of a single conduction path, the conductivity will have the same form as Eq. (2), but with an effective threshold field  $\hat{E}_T = \sum_i E_T^i$  and effective conductivity  $\hat{\sigma}_c = (\sum_i (\sigma_c^i)^{-1})^{-1}$ . The total charge density modulation conductivity is then given by

$$\sigma_{cdm}(E) = \sum_j \hat{\sigma}_c^j \frac{E - \hat{E}_T^j}{E} \theta(E - \hat{E}_T^j), \quad (3)$$

where  $j$  runs over the parallel conduction pathways, each having their own effective threshold field  $\hat{E}_T^j$  and effective conductivity  $\hat{\sigma}_c^j$ . If there are a large number of conduction paths, the above summation can be replaced by an integration, from zero to infinity, weighted by the statistical distribution of threshold fields and conductivities. For simplicity, we assume a lorentzian distribution of width  $\gamma$ , centered on  $E_T^0$  for the threshold fields, and a constant effective conductivity  $\sigma_c^j = \hat{\sigma}_c$  for each path. The total conductivity, including the free carrier contribution,  $\sigma_0$ , can then be equated as

$$\sigma(\epsilon) = \sigma_0 + \hat{\sigma}_c \frac{2\epsilon(\arctan(\epsilon) + \arctan(\epsilon_0)) - \ln\left(\frac{1+\epsilon^2}{1+\epsilon_0^2}\right)}{(\epsilon + \epsilon_0)(\pi + 2\arctan(\epsilon_0))}, \quad (4)$$

with  $\epsilon_0 = \hat{E}_T^0/\gamma$ ,  $\epsilon = (E - \hat{E}_T^0)/\gamma$ . In the limit  $\gamma/\hat{E}_T^0 \gg 1$ , which is valid for the present experiment, the total conductivity becomes:

$$\sigma(\epsilon) = \sigma_0 + \hat{\sigma}_c \frac{2\epsilon \arctan(\epsilon) - \ln(1 + \epsilon^2)}{\epsilon\pi}, \quad (5)$$

where  $\epsilon = E/\gamma$

In the derivation of Eq. (5) quite a few assumptions have been made. The most important one is that domains are formed in the charge density modulation material, within which the charge density modulation transport is coherent. This is mainly based on the observation of the slow onset of the moving conductivity in  $\beta$ - $\text{Na}_{0.33}\text{V}_2\text{O}_5$  (see Fig. 3. and Fig. 4.) as well as in for instance  $\text{K}_{0.3}\text{MoO}_3$  [10]. The assumption of parallel paths of series resistors is pretty robust; allowing for connectivity between these paths would only lead to additional parallel pathways for conduction. Of course, there is nothing known on the statistical distribution of domain properties. Taking a symmetric lorentzian (or gaussian) distribution simply makes the integration over domains tractable. Taking an asymmetric distribution would be more physical. Also typical domain sizes are not known. X-ray diffraction measurements [38], however, have shown that the width of the superstructure peaks originating from charge ordering is comparable to the sharpness of the fundamental peaks, thereby setting a lower limit of the domain sizes to  $\sim 100$  nm. Finally, we did not allow for a distribution of effective conductivities for the conduction paths. Numerical simulations taking lorentzian distributions  $\hat{\sigma}_c^j$  have shown, however, that the shape of the field dependent conductivity does not strongly depend on this.

Now return to the data in Fig. 4. We have fitted Eq. (5) to the field dependent conductivities, measured at different temperatures between 65 K and 136 K. Note that the only free parameters in the fits are the width of the distribution  $\gamma$ , and the charge density modulation conductivity  $\hat{\sigma}_c$ , since the normal conductivity,  $\sigma_0$ , can be obtained directly from the low field data. At low temperatures, a good approximation of  $\hat{\sigma}_c$  can be made using the field dependent conductivity data taking the conductivity difference between the ohmic regime and the saturation regime. The only remaining fit parameter in this situation is the width of the lorentzian distribution,  $\gamma$ . The fits generally show a good agreement with the data, and some typical results of the fitting are shown in Fig. 6.

The temperature dependence of the threshold field distribution width,  $\gamma$ , obtained from the fits is displayed in Fig. 7.

At low temperature, the width increases with increasing temperature. It shows a pronounced peak at 80 K, after which it starts to decrease becoming very small in the region of the MI transition. The decrease with increasing temperature observed above 80 K is what one might intuitively expect; the enhanced screening will decrease the typical domain threshold fields, thereby decreasing  $\gamma$ . Apart from the decrease of the average pinning potential, there will also be changes in the statistical distribution as the temperature is lowered. At low temperatures one expects that there will be a larger number of domains with a relatively small pinning potential, reducing the distribution width. Therefore we believe that the increase of the width observed in the low temperature results from a competition of enhanced screening and the formation of larger, more strongly pinned, domains due to the coales-

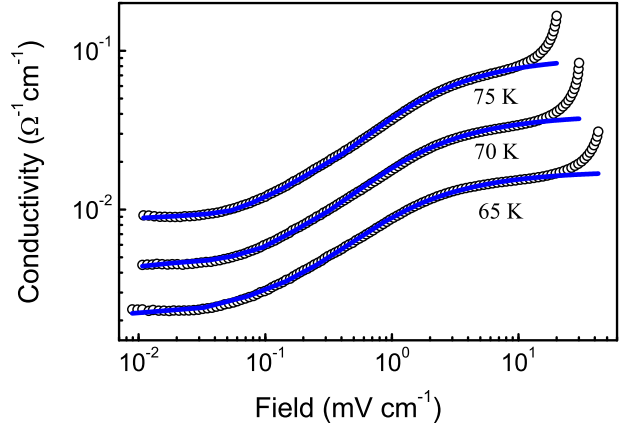


**Fig. 6.** Fits of the domain model, Eq. (5) (solid lines), to the nonlinear transport data (open symbols) at 65 K, 70 K and 75 K.

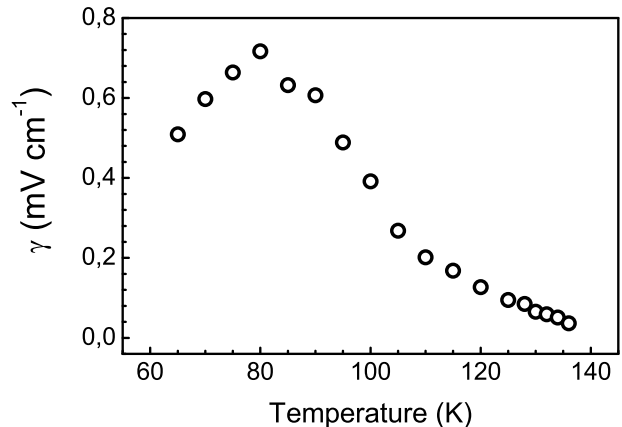


**Fig. 7.** Temperature dependence of the width  $\gamma$  of the lorentzian threshold field distribution obtained from fits of the data in Fig. 4. to the domain model, Eq. (5).

cence of small, weakly pinned, domains as the temperature increases.

Figure 8 shows the temperature dependence of the effective charge density modulation conductivity,  $\hat{\sigma}_c$ , and the low field ohmic conductivity,  $\sigma_0$ . The moving charge density modulation conductivity is found to be almost an order of magnitude larger than the quasiparticle contribution. The small kink in the charge density modulation contribution around 90 K, which probably again results from the competition between screening and coalescence.

The temperature dependence of both contributions show a similar activated behavior. For the quasiparticles this has already been discussed in section 2. The usual interpretation of the activated behavior of the moving density modulation contribution is in terms of thermally activated flux creep [35], similar to the flux creep of the Abrikosov flux lattice in superconductors [39]. From fits

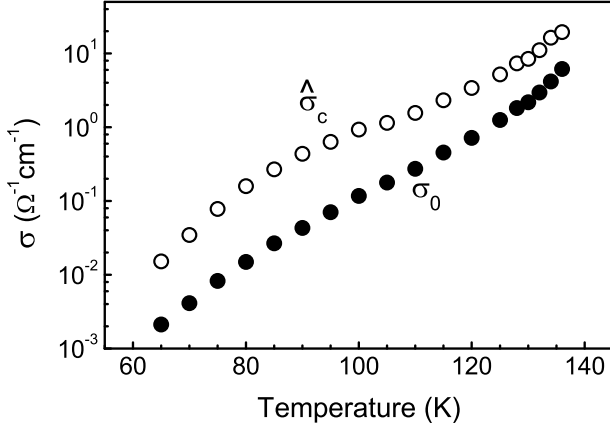


**Fig. 8.** Temperature dependence of the effective charge density modulation conductivity,  $\hat{\sigma}_c$  (open symbols), and the low field ohmic conductivity  $\sigma_0$  (filled symbols), obtained from fits of the data in Fig. 4. to the domain model, Eq. (5) (see text).

to an activated behavior we estimate the low temperature ( $T < 90$  K) activation energies for the quasiparticle and the moving density modulation contributions to be 740 K and 805 K, respectively. For the ohmic contribution, this is in good agreement with the earlier results (Sec. 2).

The above discussed model gives a phenomenological understanding of the ohmic and incoherent transport regimes. It does not, however, describe the coherent transport regime, where a sharp rise in conductivity takes place. The appearance of this second threshold field can be understood as follows. As the field increases, more and more local pinning potentials will be overcome, increasing the number of domains which contribute to the conductivity. Eventually this will lead to the formation of a percolation path between the contacts. We thus propose that the second threshold is in fact a percolation threshold. For fields bigger than the second threshold field,  $E_T^*$ , the CDW will then coherently move along such percolation paths, leading to the sharp rise in conductivity. This leads to an additional contribution to the conductivity of the form of Eq. (4), so that the total conductivity now becomes

$$\sigma(\epsilon) = \sigma_0 + \hat{\sigma}_c \frac{2\epsilon \arctan(\epsilon) - \ln(1 + \epsilon^2)}{\epsilon\pi} + \hat{\sigma}_p \frac{2\epsilon_p(\arctan(\epsilon_p) + \arctan(\epsilon_{0p})) - \ln\left(\frac{1 + \epsilon_p^2}{1 + \epsilon_{0p}^2}\right)}{(\epsilon_p + \epsilon_{0p})(\pi + 2 \arctan(\epsilon_{0c}))} \quad (6)$$

where  $\epsilon_p = (E - E_T^*)/\gamma_p$ , and  $\epsilon_{0p} = E_T^*/\gamma_p$ .  $\gamma_p$  and  $\hat{\sigma}_p$  are the width of the distribution and the percolation charge density modulation conductivity, respectively. We have fitted this last equation to the low temperature ( $T < 90$  K) field dependent conductivities and some typical results of the fitting are shown in Fig. 9.

Clearly the data follows Eq. (6) quite well. The temperature dependence of the upper threshold field (see inset Fig. 9.) closely follows the results presented in Fig. 5. The

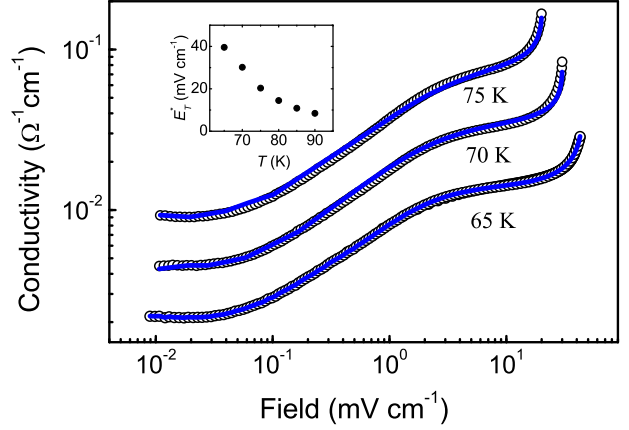


**Fig. 9.** Fits of the domain-percolation model, Eq. (3) (solid lines) to the nonlinear transport data (open symbols) at 65 K, 70 K and 75 K. The inset shows the behavior of the percolation threshold with temperature.

reason for the sharp decrease of the percolation threshold field upon increasing temperature is the same as for the incoherent moving threshold, as has been discussed in section 2, namely the increased screening of impurities upon increasing temperature. Finally, we note that the fitting is fairly insensitive to the distribution width as long as  $\gamma_p \ll E_T^*$ , as expected for a percolation threshold.

## 4 Conclusions

We presented detailed nonlinear transport experiments on  $\beta$ - $\text{Na}_{0.33}\text{V}_2\text{O}_5$  in the temperature range 30 K - 300 K. The low field data in the charge ordered phase show that two types of excitations contribute to the transport. The charge density modulation quasiparticle gap is found to be about 700-800 K, and likely depends on the sodium stoichiometry. Evidence for a second type of excitation, with a gap of  $\sim 500$  K, has been presented, although the exact origin of this excitation remains unclear at present. It might be either a bound state of collective charge density modulation excitations like the phason, or possibly an excitation within the domain walls between ordered charge density modulation domains. A competing model for the thermally activated low field charge transport in a low dimensional system in the presence of disorder is the variable range hopping (VRH) model [40,41]. Analyzing the low temperature data in terms of VRH conductivity indeed leads to a reasonable agreement with this model as well, again with deviations at temperatures below 50 K. Since the present data can not distinguish between these models we adapted the most widely used model here as well.

The field dependent data clearly show the charge density modulation nature of the insulating phase, and is very similar to the transport in other well known charge density modulation materials like  $\text{K}_{0.3}\text{MoO}_3$ . The phenomenolog-

ical domain model for nonlinear transport in charge density modulation materials presented here is found to be in good agreement with the experiments, and we believe that this model should be applicable to other semi-conducting charge ordered materials as well. The model could be improved by taking a more realistic model for the statistical distribution of domain properties, the single domain transport, and by allowing for field dependent domain properties. In particular the pinning fields are expected to be field dependent, since at high moving velocities the charge density modulation excitations may excite quasiparticle excitations resulting from charge density friction. Finally, we believe that in low free carrier density (*i.e.* semiconducting) compounds like  $\beta$ - $\text{Na}_{0.33}\text{V}_2\text{O}_5$  and  $\text{K}_{0.3}\text{MoO}_3$  much of the temperature dependence of the transport properties, including the observed decrease of threshold fields upon raising temperature, can be understood in terms of enhanced screening of pinning centers by thermally excited charge carriers.

Acknowledgements – This project is supported by the Netherlands Foundation for Fundamental Research on Matter with financial aid from the Nederlandse Organisatie voor Wetenschappelijk Onderzoek.

## References

1. G. Grüner, Rev. Mod. Phys. **60**, 1129 (1988).
2. J. Dumas, C. Schlenker, J. Marcus and R. Buder, Phys. Rev. Lett. **50**, 757 (1983).
3. R. M. Fleming and C. C. Grimes, Phys. Rev. Lett. **42**, 1423 (1979).
4. Marko Pinteric, N. Biskup and Silvia Tomic and J. U. von Schutz, Synth. Metals **103**, 2185 (1999).
5. Z. Z. Wang, J. C. Girard, C. Pasquier, D. Jerome and K. Bechgaard, Phys. Rev. B **67**, 121401 (2003).
6. R. E. Peierls, *Quantum Theory of solids* (Calderon, Oxford 1955) 108.
7. N. P. Ong and P. Monceau, Phys. Rev. B **16**, 3443 (1977).
8. Ayan Guha, Arindam Ghosh, A. K. Raychaudhuri, S. Parashar, A. R. Raju and C. N. R. Rao, Appl. Phys. Lett. **75**, 3381 (1999).
9. S. Brazovskii and T. Nattermann, Adv. in Phys. **53**, 177 (2004).
10. P. H. M. van Loosdrecht, B. Beschoten, I. Dotsenko and S. van Smaalen, J. Phys. IV France **12**, 303 (2002).
11. B. Zawilski, J. Marcus and T. Klein, Europh. Lett. **50**, 75 (2000).
12. G. X. Tessema and L. Mihaly, Phys. Rev. B **35**, 7680 (1987).
13. H. Yamada and Y. Ueda, J. Phys. Soc. Jpn. **68**, 2735 (1999).
14. T. Yamauchi, Y. Ueda and N. Mori, Phys. Rev. Lett. **89**, 057002 (2002).
15. M. J. Sienko and J. B. Sohn, J. of Chem. Phys. **44**, 1369 (1965).
16. Yasuyuki Kanai, Seiichi Kagoshima and Hiroshi Nagasawa, Jour. Phys. Soc. Jpn. **51**, 697 (1982).
17. Y. Ueda, H. Yamada, M. Isobe and T. Yamauchi, J. Alloys and Compounds **317**, 109 (2001).
18. S. Nagai, M. Nishi, K. Kakurai, Y. Oohara, H. Kimura, Y. Noda, T. Yamauchi, J. I. Yamaura, M. Isobe, Y. Ueda and K. Hirota, J. Phys. Soc. Jpn., **74**, 1297 (2005).
19. C. Presura, M. Popinciuc, P. H. M. van Loosdrecht, D. van der Marel and M. Mostovoy, Phys. Rev. Lett. **90**, 026402 (2003).
20. C. Presura, *Energetics and ordering in strongly correlated oxides as seen in optics*, Ph. D. Thesis, University of Groningen, The Netherlands, 2003.
21. The values of the resistivity at a given temperature differ slightly for different samples, presumably due to small variations in the sodium stoichiometry [13].
22. S. A. Brazovskii, Sov. Phys. JETP **51**, 342 (1980).
23. The electric field is defined as the measured voltage divided by the probe contact separation.
24. G. Mihály, P. Beauchene, J. Marcus, J. Dumas and C. Schlenker, Phys. Rev. B **37**, 1047 (1988).
25. R. M. Fleming, R. J. Cava, L. F. Schneemeyer, E. A. Rieterman and R. G. Dunn, Jour. Phys. Rev. B. **33**, 5450 (1986).
26. Dingli Wang, Qingming Xiao, Wufeng Tang, Tongyun Zhao, Jing Shi, Decheng Tian and Mingliang Tian, Modern Phys. Lett. B. **13**, 109 (1999).
27. P. Beauchene, J. Dumas, A. Janossy, J. Marcus and C. Schlenker, Physica B **143**, 126 (1986).
28. S. Yue, C. A. Kuntscher, M. Dressel, S. van Smaalen, F. Ritter and W. Assmus, cond-mat/0501332.
29. C. Schlenker, *Low-Dimensional Electronic Properties of Molybdenum Bronzes and Oxides* (Kluwer Academic Publishers, 1989).
30. H. Frölich, Proc. R. Soc. A **223**, 296 (1954).
31. N. Ogawa, K. Miyano and S. Brazovski, Phys. Rev. B **71**, 075118 (2005).
32. P. Monceau, J. Richard and M. Renard, Jour. Phys. Rev. B. **25**, 931 (1982).
33. G. Grüner, A. Zawadowski and P.M. Chaikin, Phys. Rev. Lett. **46**, 511 (1981).
34. J. Bardeen, Phys. Rev. Lett. **42**, 1498 (1979).
35. S. G. Lemay, R. E. Thorne, Y. Li and J. D. Brock, Phys. Rev. Lett. **83**, 2793 (1999).
36. H. Fukuyama and P. A. Lee, Phys. Rev. B. **17**, 535 (1978).
37. P. A. Lee and T. M. Rice, Phys. Rev. B. **19**, 3970 (1979).
38. J. I. Yamaura, M. Isobe, H. Yamada, T. Yamauchi and Y. Ueda, J. of Phys. and Chem. of Solids **63**, 957 (2002).
39. P. W. Anderson and Y. B. Kim, Rev. Mod. Phys. **36**, 39 (1964).
40. N. F. Mott, Philos. Mag. **19**, 835 (1969).
41. N. F. Mott and E. A. Davis, *Electronic Processes in Non-Crystalline Materials* (Clarendon Press, Oxford 1979).